

2 **First Neutrino-Induced-Muon Momentum** 3 **Determination by Multiple Coulomb Scattering in a** 4 **LArTPC**

5 **The MicroBooNE Collaboration**

6 ABSTRACT: Liquid Argon Time Projection Chambers (LArTPCs) are an important detector tech-
7 nology for the future of neutrino physics. This technology provides precise three-dimensional
8 reconstruction of charged particle tracks that traverse the detector medium. We discuss a technique
9 for measuring a charged particle's momentum by means of multiple coulomb scattering (MCS) in
10 the MicroBooNE LArTPC, which does not require the full particle ionization track to be contained
11 inside of the detector volume as other track momentum reconstruction methods do (range-based
12 momentum reconstruction and calorimetric momentum reconstruction). We provide motivation for
13 why this technique is important, and quantify its performance on fully contained beam-neutrino-
14 induced muon tracks both in simulation and in data. In general we find agreement between data
15 and simulation, with small bias in the momentum reconstruction and with resolutions that vary as
16 a function of track length, decreasing from about 11% for the shortest (one meter long) tracks to
17 nearly 5% for longer (several meter) tracks. Quantification of the performance on exiting tracks, or
18 tracks which are higher energy than those which are fully contained, will be determined in a future
19 publication.

20	Contents	
21	1 Introduction and Motivation	1
22	2 Multiple Coulomb Scattering (MCS)	3
23	3 MCS Implementation Using the Maximum Likelihood Method	4
24	3.1 Track Segmentation and Scattering Angle Computation	4
25	3.2 Maximum Likelihood Theory	5
26	3.3 Maximum Likelihood Implementation	5
27	4 Range-based Energy Validation from Simulation	6
28	5 MCS Performance on Beam Neutrino-Induced Muons in MicroBooNE Data	6
29	5.1 Input Sample	6
30	5.2 Event Selection	7
31	5.3 Highland Validation	8
32	5.4 MCS Momentum Validation	8
33	6 Conclusions	11

34 1 Introduction and Motivation

35 MicroBooNE (Micro Booster Neutrino Experiment) is an R&D experiment based at the Fermi Na-
36 tional Accelerator Laboratory (Fermilab) that uses a large Liquid Argon Time Projection Chamber
37 (LArTPC) to investigate the excess of low energy events observed by the MiniBooNE experiment
38 [1] and to study neutrino-argon cross-sections. MicroBooNE is part of the Short-Baseline Neutrino
39 (SBN) physics program, along with two other LArTPCs: the Short Baseline Near Detector (SBND)
40 and the Imaging Cosmic And Rare Underground Signal (ICARUS) detector. MicroBooNE also
41 provides important research and development in terms of detector technology and event recon-
42 struction techniques for future LArTPC experiments including DUNE (Deep Underground Neu-
43 trino Experiment).

44
45 The MicroBooNE detector[2] consists of a rectangular time projection chamber (TPC) with
46 dimensions 2.6 m width \times 2.3 m height \times 10.4 m length located 470 m away from the Booster
47 Neutrino Beam (BNB) target. LArTPCs allow for precise three-dimensional reconstruction of par-
48 ticle interactions. The x - direction of the TPC corresponds to the drift coordinate, the y - direction
49 is the vertical direction, and the z - direction is the direction along the beam. The mass of active
50 liquid argon in the MicroBooNE TPC is 89 tons, with the total cryostat containing 170 tons of
51 liquid argon.

52

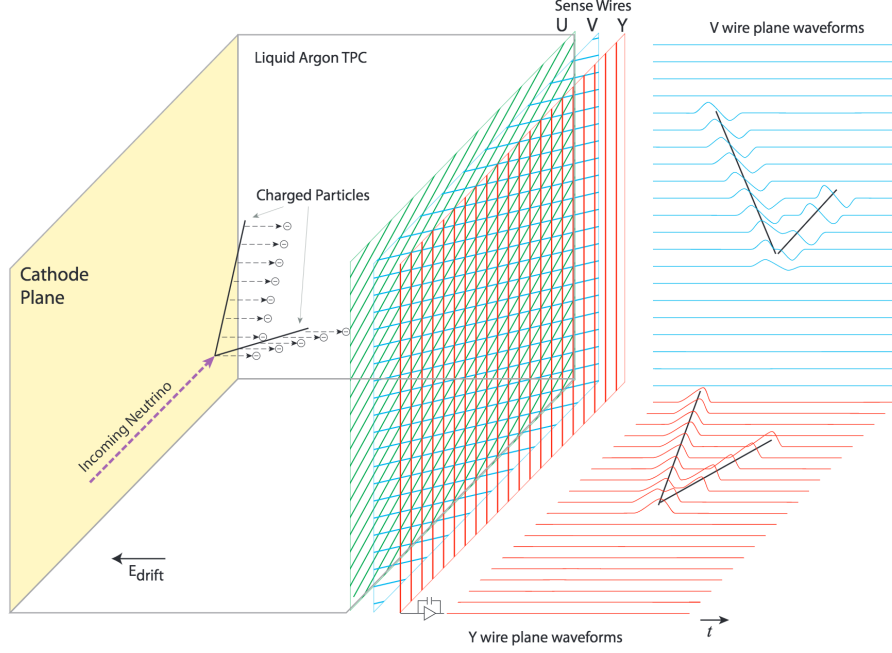


Figure 1. A diagram of the time projection chamber of the MicroBooNE detector [3].

53 A set of 32 photomultiplier tubes (PMTs) and three wire planes with 3 mm spacing at angles of
 54 0, and ± 60 degrees with respect to the vertical are located in the TPC for event reconstruction (Fig-
 55 ure 1), and the cathode plane operating voltage is -70 kV. In a neutrino interaction, a neutrino from
 56 the beam interacts with an argon nucleus and the charged outgoing secondary particles traverse the
 57 medium, losing energy and leaving an ionization trail. The resulting ionization electrons drift to the
 58 anode side of the TPC, containing the wire planes. The passage of these electrons near the first two
 59 wire planes induces a signal in them and their collection on the third plane also generates a signal.
 60 These signals are used to create three distinct two-dimensional views (in terms of wire and time)
 61 of the event. Combining these wire signals with timing information from the PMTs allows for full
 62 three-dimensional reconstruction of the event. The fiducial volume used in this analysis is defined
 63 as the full TPC volume reduced by 20 cm from both the cathode plane and the anode wire planes,
 64 by 26.5 cm from both the top and bottom walls of the TPC, by 20 cm from the beam-upstream wall
 65 of the TPC, and by 36.8 cm from the beam-downstream wall of the TPC, which corresponds to a
 66 mass of 55 tons.

67

68 The Booster Neutrino Beam (BNB) is predominantly composed of muon neutrinos (ν_μ) with
 69 a peak neutrino energy of about 0.7 GeV, which can undergo charge-current (ν_μ CC) interactions
 70 in the TPC and produce muons. For muon tracks that are completely contained in the TPC, it is
 71 straightforward to calculate their momentum with a measurement of the length of the particle's

track, or with calorimetric measurements which come from wire signal measurements. However, around half of muons from BNB neutrino events in MicroBooNE are not fully contained in the TPC, and therefore using length-based calculations for these uncontained tracks is not a possibility. The only way to compute the energy of a non-contained three-dimensional track is by means of multiple coulomb scattering (MCS).

In this paper we describe the theory behind multiple coulomb scattering and a maximum likelihood based algorithm that is used to determine the momentum of particles in a LArTPC. That this technique works and is valid for a sample of fully contained muons from BNB ν_μ CC interactions is demonstrated, with bias and resolutions quantified. Quantification of the performance on exiting tracks, or tracks which are higher energy than those which are fully contained, will be determined in a future publication.

2 Multiple Coulomb Scattering (MCS)

Multiple Coulomb Scattering (MCS) occurs when a charged particle enters a medium and undergoes electromagnetic scattering with the atomic nuclei. This scattering deviates the original trajectory of the particle within the material (Figure 2). For a given energy, the angular deflection scatters of a particle in either the x' direction or y' direction (as indicated in the aforementioned figure) form a gaussian distribution centered at zero with a width, σ_o^{HL} given by the Highland formula [4]:

$$\sigma_o^{HL} = \frac{13.6 \text{ MeV}}{p\beta c} z \sqrt{\frac{\ell}{X_0}} \left[1 + 0.0038 \ln\left(\frac{\ell}{X_0}\right) \right] \quad (2.1)$$

where β is the ratio of the particle's velocity to the speed of light, ℓ is the distance traveled inside the material, z is the magnitude of the charge of the particle, and X_0 is the radiation length of the target material (taken to be a constant 14 cm in liquid argon). In practice, a modified version of the Highland formula is used

$$\sigma_o = \sqrt{(\sigma_o^{HL})^2 + (\sigma_o^{res})^2} = \sqrt{\left(\frac{13.6 \text{ MeV}}{p\beta c} z \sqrt{\frac{\ell}{X_0}} \left[1 + 0.0038 \ln\left(\frac{\ell}{X_0}\right) \right]\right)^2 + (\sigma_o^{res})^2} \quad (2.2)$$

where the formula is “modified” from the original Highland formula (Equation 2.1) in that it includes a detector-inherent angular resolution term, σ_o^{res} . For this analysis, this term is given a fixed value of 2 mrad which has been determined to be an acceptable value based on simulation studies (varying this term widely has negligible impact on the algorithm performance on the sample of tracks studied in this note).

With the Highland formula, the momentum of a track-like particle can be determined using only the 3D reconstructed track it produces in the detector, without any calorimetric or track range information. Within neutrino physics, past emulsion detectors like the DONUT [5] and OPERA [6] experiments have used MCS to determine particle momenta. Additionally, the MACRO [7] experiment at Gran Sasso Laboratory utilized this technique as well. While the original method for

106 using MCS to determine particle momentum in a LArTPC involved using a Kalman Filter and was
 107 described by the ICARUS collaboration [8], the maximum-likelihood based method discussed in
 108 this paper for use in the MicroBooNE detector is described in detail in Section 3.

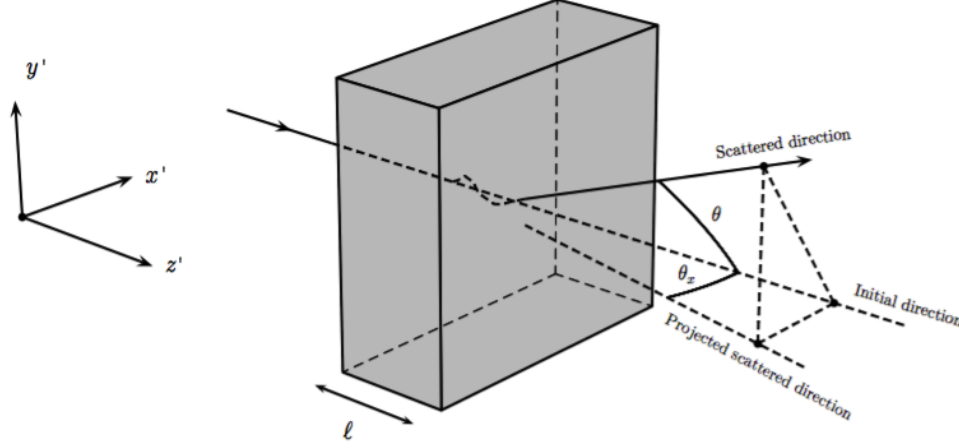


Figure 2. The particle's trajectory is deflected as it traverses through the material.

109 3 MCS Implementation Using the Maximum Likelihood Method

110 This section describes exactly how the phenomenon of multiple coulomb scattering is leveraged
 111 to determine the momentum of a track-like particle reconstructed in a LArTPC. In general, the
 112 approach is as follows:

- 113 1. The three-dimensional track is divided into segments of configurable length.
- 114 2. The scattering angles between consecutive segments are measured.
- 115 3. Those angles combined with the modified Highland formula (Equation 2.2) are used to build
 116 a likelihood that the particle has a specific momentum, taking into account energy loss in
 117 upstream segments of the track.
- 118 4. The momentum corresponding to the maximum likelihood is chosen to be the MCS com-
 119 puted momentum.

120 Each of these steps are discussed in detail in the following subsections.

122 3.1 Track Segmentation and Scattering Angle Computation

123 Track segmentation refers to the subdivision of three-dimensional reconstructed trajectory points
 124 of a reconstructed track into portions of definite length. In this analysis, the tracks are automati-
 125 cally reconstructed by the “pandoraNuPMA” projection matching algorithm which constructs the
 126 three-dimensional trajectory points by combining two-dimensional hits reconstructed from signals

on the different wire planes along with timing information from the photomultiplier tubes to reconstruct the third dimension [9]. The segmentation routine begins at the start of the track, and iterates through the trajectory points in order, defining segment start and stop points based on the straight-line distance between them. There is no overlap between segments. Given the subset of the three-dimensional trajectory points that correspond to one segment of the track, a three-dimensional linear fit is applied to the data points, weighting all trajectory points equally in the fit. In this analysis, a segment length of 10 cm is used, which is a tunable parameter that has been optimized based on simulation studies.

With the segments defined, the scattering angles between adjacent segments are computed. A coordinate transformation is performed such that the z' direction is oriented along the direction of the first of the segment pair. The x' and y' coordinates are then defined such that all of x' , y' , and z' are mutually orthogonal, as shown in Figure 2. The scattering angles both with respect to the x' direction and the y' direction are then computed to be used by the MCS algorithm. Note that only the scattering angle with respect to the x' direction is drawn in Figure 2.

3.2 Maximum Likelihood Theory

The normal probability distribution for the scattering angle in either the x' or y' direction, $\Delta\theta$ with an expected gaussian error σ_o and mean of zero is given by:

$$f_X(\Delta\theta) = (2\pi\sigma_o^2)^{-\frac{1}{2}} \exp\left(-\frac{1}{2}\left(\frac{\Delta\theta}{\sigma_o}\right)^2\right) \quad (3.1)$$

Here, σ_o is the RMS angular deflection computed by the modified Highland formula (Equation 2.2), which is a function of both the momentum and the length of that segment. Since energy is lost between segments along the track, σ_o increases for each angular measurement along the track so we replace σ_o with $\sigma_{o,j}$, where j is an index representative of the segment.

To get the likelihood, one takes the product of $f_X(\Delta\theta_j)$ over all n of the $\Delta\theta_j$ segment-to-segment scatters along the track. With some manipulation, this product becomes

$$L((\sigma_{o,1})^2, \dots, (\sigma_{o,n})^2; \Delta\theta_1, \dots, \Delta\theta_n) = (2\pi)^{-\frac{n}{2}} \times \prod_{j=1}^n (\sigma_{o,j})^{-1} \times \exp\left(-\frac{1}{2} \sum_{j=1}^n \left(\frac{\Delta\theta_j}{\sigma_{o,j}}\right)^2\right) \quad (3.2)$$

In practice, rather than maximizing likelihood it is often more computationally convenient to instead minimize the negative log likelihood. Inverting the sign and taking the natural logarithm of the likelihood L gives an expression that is related to a χ^2

$$-l(\mu_o; (\sigma_{o,1})^2, \dots, (\sigma_{o,n})^2; \Delta\theta_1, \dots, \Delta\theta_n) = -\ln(L) = \frac{n}{2} \ln(2\pi) + \sum_{j=1}^n \ln(\sigma_{o,j}) + \frac{1}{2} \sum_{j=1}^n \left(\frac{\Delta\theta_j}{\sigma_{o,j}}\right)^2 \quad (3.3)$$

3.3 Maximum Likelihood Implementation

Given a set of angular deflections in the x' and y' directions for each segment as described in Section 3.1 a raster scan over postulated track momenta in steps of 1 MeV up to 7.5 GeV is computed and the step with the smallest negative log likelihood (Equation 3.3) is chosen as the final

159 MCS momentum. Note that Equation 3.3 includes a $\sigma_{o,j}$ term which changes for each consecutive
 160 segment because their energies are decreasing. The energy of the j th segment is given by

$$E_j = E_t - k_{cal} * N_{upstream} * l_{seg} \quad (3.4)$$

161 where k_{cal} is the minimally ionizing energy constant taken to be $2.105 \frac{MeV}{cm}$ in liquid argon
 162 [10], $N_{upstream}$ is the number of segments upstream of the j th segment, and l_{seg} is the 3D segment
 163 length. This definition of E_j therefore takes into account energy loss along the track. Note that
 164 Equation 3.4 introduces a minimum allowable track energy determined by the length of the track,
 165 as E_j must remain positive. This value of segment energy is converted to a momentum, p , with the
 166 usual energy-momentum relation, assuming the muon mass, and is then used to predict the RMS
 167 angular scatter for that segment (σ_o) by way of Equation 2.2.

168 4 Range-based Energy Validation from Simulation

169 In order to quantify the performance of the MCS energy estimation method on fully contained
 170 muons in data, an additional handle on energy is needed. Here, range-based energy is used.
 171 The stopping power of muons in liquid argon is well described by the continuous-slowing-down-
 172 approximation (CSDA) by the particle data group (PDG) with agreement to data at the sub-percent
 173 level [10] [11] [12]. By using a linear interpolation between points in the cited PDG stopping power
 174 table, the length of a track can be used to reconstruct the muon's total energy with good accuracy.
 175 A simulated sample of fully contained BNB neutrino-induced muons longer than one meter is used
 176 to quantify the bias and resolution for the range-based energy estimation technique. The range is
 177 defined as the straight-line distance between the true starting point and true stopping point of a
 178 muon. The bias and resolution are computed in bins of true total energy of the muons by fitting a
 179 gaussian to a distribution of the fractional energy difference ($\frac{E_{Range} - E_{True}}{E_{True}}$) in each bin. The mean
 180 of each gaussian indicates the bias for that true energy bin, and the width indicates the resolution.
 181 Figure 3 shows the bias and resolution for the range-based energy reconstruction method. It can be
 182 seen that the bias is negligible and the resolution for this method of energy reconstruction is on the
 183 order of 2-4%. Based on this figure, it is clear that range-based energy (and therefore range-based
 184 momentum) is a good handle on the true energy (momentum) of a reconstructed muon track in
 185 data, assuming that the track is well reconstructed in terms of length.

186 5 MCS Performance on Beam Neutrino-Induced Muons in MicroBooNE Data

187 5.1 Input Sample

188 The input sample to this portion of the analysis is $\sim 5e19$ protons-on-target worth of triggered
 189 BNB neutrino interactions in MicroBooNE data, which is a small subset of the nominal amount
 190 of beam scheduled to be delivered to the detector. These events are run through a fully automated
 191 reconstruction chain which produces reconstructed objects including three-dimensional neutrino
 192 interaction points (vertices), three-dimensional tracks for each outgoing secondary particle from
 193 the interaction, and PMT-reconstructed optical flashes from the interaction scintillation light. The
 194 fiducial volume used in this analysis is defined in Section 1.

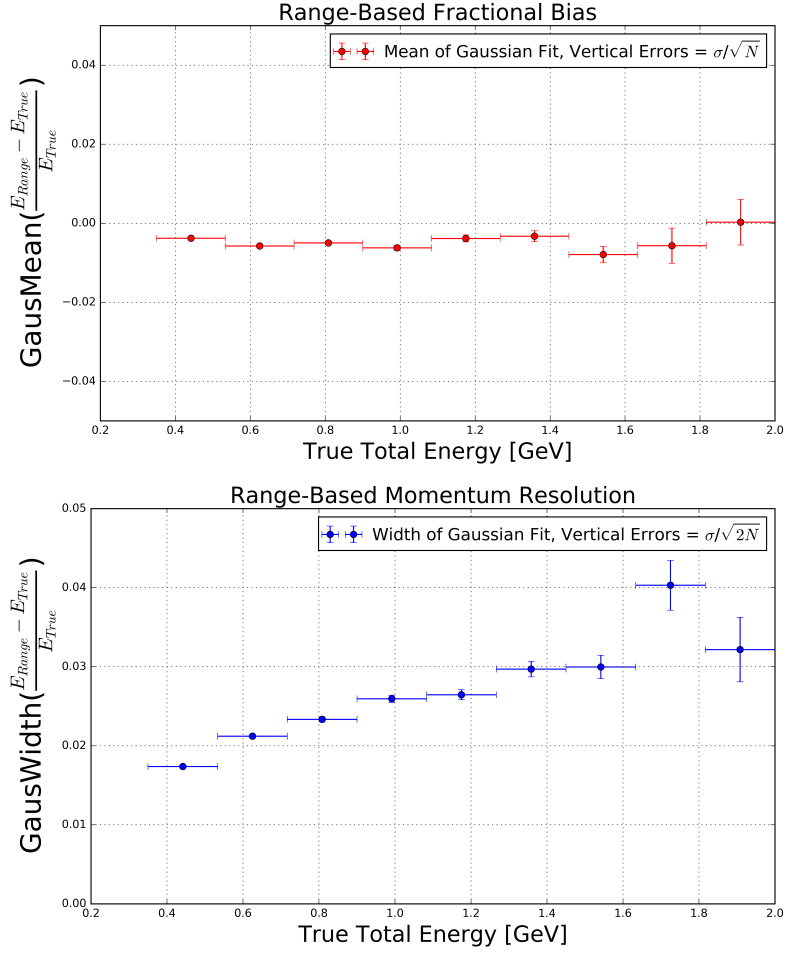


Figure 3. Range-based energy fractional bias (top) and resolution (bottom) from a sample of simulated fully contained BNB neutrino-induced muons using true starting and stopping positions of the track. The bias is less than 1% and the resolution is below $\approx 4\%$.

5.2 Event Selection

The following selection cuts are placed on the aforementioned reconstructed objects to select ν_μ charged-current interactions in which the muon track exiting the interaction vertex is fully contained within the fiducial volume:

1. The event must have at least one bright optical flash in coincidence with the expected BNB neutrino arrival time.
2. Two or more reconstructed tracks must originate from the same reconstructed vertex within the fiducial volume.
3. The span in z - of the track must be within 70 cm of the z - position of the optical flash as determined by the pulse height and timing of signals in the 32 PMTs.

- 205 4. For events with exactly two tracks originating from the vertex, additional calorimetric-based
206 cuts are applied to mitigate backgrounds from in-time cosmics which produce Michel elec-
207 trons that are reconstructed as a track.
- 208 5. The longest track originating from the vertex is assumed to be a muon, and it must be fully
209 contained within the fiducial volume.
- 210 6. The longest track must be at least one meter long, in order to have enough sampling points
211 in the MCS likelihood to obtain a reasonable estimate of its momentum.

212 In this sample of MicroBooNE data, 598 events (tracks) remain after all event selection cuts.
213 The relatively low statistics in this sample is due to the limited input sample, described in Sec-
214 tion 5.1. Each of these events (tracks) were scanned by hand with a 2D interactive event display
215 showing the raw wire signals of the interaction from each wire plane, with the 2D projection of the
216 reconstructed muon track and vertex overlaid. The scanning was done to ensure the track was well
217 reconstructed with start point close to the reconstructed vertex and end point close to the end of the
218 visible wire-signal track in all three planes. Additionally the scanning was to remove obvious mis-
219 identification (MID) topologies such as cosmic rays inducing Michel electrons at the reconstructed
220 neutrino vertex which were not successfully removed by the automated event selection cuts. After
221 rejecting events (tracks) based on hand scanning, 396 tracks remain for analysis.

222 5.3 Highland Validation

223 The Highland formula indicates that histogram of track segment-by-segment angular deviations
224 in both the x' and y' directions divided by the width predicted from the Highland equation σ_o^{HL}
225 (Equation 2.1) should be gaussian with a width of unity. In order to calculate the momentum p in
226 the Highland equation, p for each segment is computed with Equation 3.4 where E_t comes from the
227 converged MCS computed momentum of the track. For each consecutive pair of segments in this
228 sample of 396 tracks, the angular scatter in milliradians divided by the Highland expected RMS in
229 milliradians is an entry in the area-normalized histogram shown in Figure 4. From this figure we
230 can see that the basis of the MCS technique is validated.

231 5.4 MCS Momentum Validation

232 The MCS momentum versus range-based momentum for this sample of 396 tracks can be seen in
233 Figure 5.

234 The MCS momentum fractional bias and resolution as a function of range-based momentum
235 for this sample of 396 tracks is shown in Figure 6. In order to compute this bias and resolution,
236 distributions of fractional inverse momentum difference ($\frac{p_{MCS}^{-1} - p_{Range}^{-1}}{p_{Range}^{-1}}$) in bins of range-based
237 momentum p_{Range} are fit to gaussians and the mean of the fit determines the bias while the width
238 of the fit determines the resolution for that bin. Inverse momentum is used here because the binned
239 distributions are more gaussian (since the Highland formula is a function of inverse momentum),
240 and therefore using the resulting fit parameters is more valid. Note that simply using the mean
241 and RMS of the binned distributions yields similar results. Also shown in this figure are the
242 bias and resolutions for an analogous simulated sample consisting of full BNB simulation with

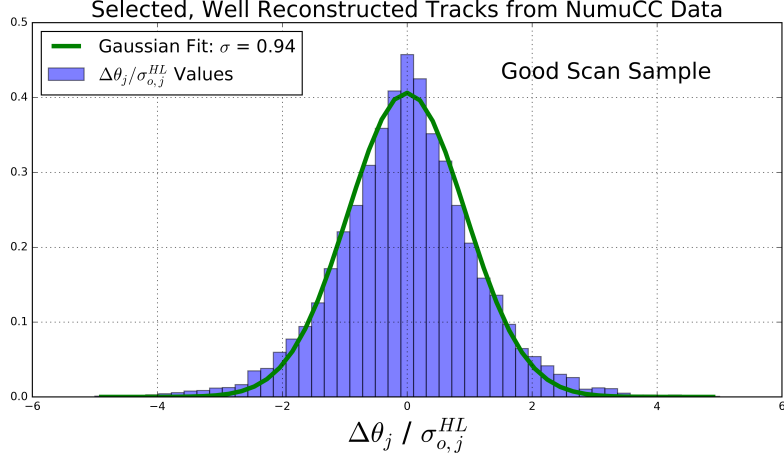


Figure 4. Segment-to-segment measured angular scatters in both the x' and y' directions divided by the Highland formula (Equation 2.1) predicted width σ_o^{HL} for the automatically selected beam neutrino-induced fully contained muon sample in MicroBooNE data after hand scanning to remove poorly reconstructed tracks and obvious mis-identification (MID) topologies. A gaussian distribution with a width of unity indicates that the basis of the MCS technique is validated.

243 CORSIKA-generated [13] cosmic overlays passed through an identical reconstruction and event
 244 selection chain. Rather than hand scanning this sample, truth-based information was used by re-
 245 quiring the longest reconstructed track matched well in terms of true starting and stopping point of
 246 the ν_μ CC muon. This removes any mis identifications or interference from the simulated cosemics.
 247 These resolutions on the order of 10% are consistent with the monte-carlo Kalman filter results
 248 presented by the ICARUS collaboration in this momentum range [8] as summarized in Table 1.
 249

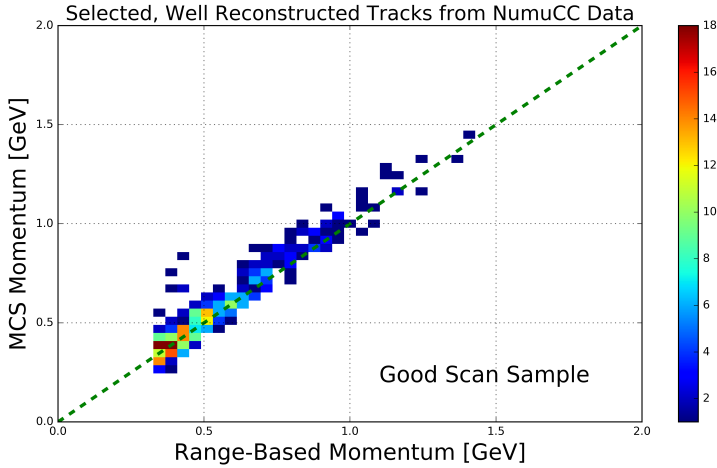


Figure 5. MCS computed momentum versus range momentum for the automatically selected beam neutrino-induced fully contained muon sample in MicroBooNE data after hand scanning to remove poorly reconstructed tracks and obvious mis-identification (MID) topologies.

Table 1. MicroBooNE maximum-likelihood based MCS fractional resolution on simulation as compared to published ICARUS Kalman Filter based MCS fractional resolution on simulation [8] as manually extrapolated from Figure 7 in the cited publication.

	$p_{true} = 0.5 \text{ GeV}$	$p_{true} = 1.0 \text{ GeV}$
ICARUS	12%	10%
MicroBooNE	9%	6%

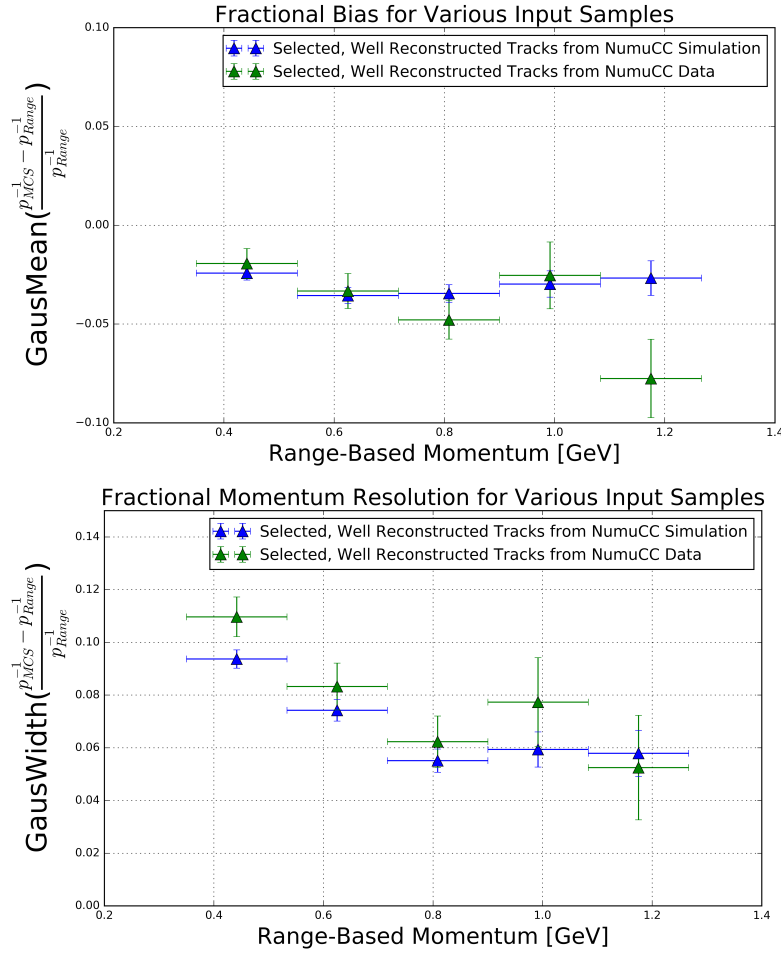


Figure 6. MCS momentum fractional bias (top) and resolution (bottom) for automatically selected contained ν_μ CC-induced muons from full simulated BNB events with cosmic overlay where the track matches with the true muon track (blue), and automatically selected contained ν_μ CC-induced muons from MicroBooNE data where the track is deemed well-reconstructed and likely-muon from hand scanning (green).

Figure 6 indicates a bias in the MCS momentum resolution on the order of a few percent, with a resolution that decreases from about 11% (9%) for contained reconstructed tracks in data (simulation) with range momentum around 0.45 GeV (which corresponds to a length of about 1.5 meters) to about 5% (6%) for contained reconstructed tracks in data (simulation) with range momentum about 1.15 GeV (which corresponds to a length of about 4.6 meters). In general bias and resolutions agree between data and simulation within uncertainty, with resolution slightly worse in data which can be attributed to the inefficiencies involved in hand scanning compared to the truth-based matching cut in simulation.

6 Conclusions

We have described the multiple coulomb scattering technique maximum likelihood method for estimating the momentum of a three dimensional reconstructed track in a LArTPC and have provided motivation for development of such a technique. This technique is a very valuable tool; it is the only way to estimate the momentum of an exiting muon and will be an important ingredient in future oscillation and cross-section measurements by MicroBooNE and within the LArTPC community as a whole. The performance of this method has been quantified both in simulation and in data on beam ν_μ CC-induced muons which are fully contained, with fractional bias less than 5% and with fractional resolution at or below 11%.

References

- [1] A. A. Aguilar-Arevalo *et al.* [MiniBooNE Collaboration], Improved Search for $\bar{\nu}_\mu \rightarrow \bar{\nu}_e$ Oscillations in the MiniBooNE Experiment, *Phys. Rev. Lett.* **110**, 161801 (2013).
doi:10.1103/PhysRevLett.110.161801 [arXiv:1207.4809 [hep-ex], arXiv:1303.2588 [hep-ex]].
- [2] R. Acciarri *et al.* [MicroBooNE Collaboration], “Design and Construction of the MicroBooNE Detector,” arXiv:1612.05824 [physics.ins-det].
- [3] S. Lockwitz, The MicroBooNE LArTPC,
<http://www-microboone.fnal.gov/talks/dpfMicroBooNELArTPC.pdf>.
- [4] V. L. Highland, Some Practical Remarks on Multiple Scattering, *Nucl. Instrum. Methods* **129** (1975) 104-120.
- [5] K. Kodama *et al.* [DONUT Collaboration], *Phys. Lett. B* **504**, 218 (2001)
doi:10.1016/S0370-2693(01)00307-0 [hep-ex/0012035].
- [6] N. Agafonova *et al.* [OPERA Collaboration], *New J. Phys.* **14**, 013026 (2012)
doi:10.1088/1367-2630/14/1/013026 [arXiv:1106.6211 [physics.ins-det]].
- [7] G. Giacomelli [MACRO Collaboration], *Braz. J. Phys.* **33**, 211 (2003)
doi:10.1590/S0103-97332003000200008 [hep-ex/0210006].
- [8] A. Ankowski *et al.* [ICARUS Collaboration], “Measurement of through-going particle momentum by means of multiple scattering with the ICARUS T600 TPC,” *Eur. Phys. J. C* **48**, 667 (2006)
doi:10.1140/epjc/s10052-006-0051-3 [hep-ex/0606006].
- [9] J. S. Marshall and M. A. Thomson, “The Pandora Software Development Kit for Pattern Recognition,” *Eur. Phys. J. C* **75**, no. 9, 439 (2015) doi:10.1140/epjc/s10052-015-3659-3 [arXiv:1506.05348 [physics.data-an]].

- 289 [10] D. E. Groom, N. V. Mokhov and S. Striganov, “Muon Stopping Power and Range Tables: 10 MeV -
290 100 TeV” Table 5, <http://pdg.lbl.gov/2012/AtomicNuclearProperties/adndt.pdf>
- 291 [11] Table 289: Muons in Liquid argon (Ar) [http://pdg.lbl.gov/2012/AtomicNuclearProperties/
292 MUON_ELOSS_TABLES/muonloss_289.pdf](http://pdg.lbl.gov/2012/AtomicNuclearProperties/MUON_ELOSS_TABLES/muonloss_289.pdf)
- 293 [12] “Stopping Powers and Ranges for Protons and Alpha Particles,” ICRU Report No. 49 (1993); Tables
294 and graphs of these data are available at <http://physics.nist.gov/PhysRefData/>
- 295 [13] D. Heck, J. Knapp, J. N. Capdevielle, G. Schatz, T. Throw, *CORSIKA: A Monte Carlo Code to
296 Simulate Extensive Air Showers*, Forschungszentrum Karlsruhe Report FZKA 6019 (1998)